

Nonlinear transport by vortex tangles in cuprate high-temperature superconductors

Rong Li and Zhen-Su She*

*State Key Laboratory for Turbulence and Complex Systems,
College of Engineering, Peking University, Beijing 100871, China*

(Dated: June 2, 2017)

A unified model of vortex tangles is proposed to describe unconventional transport in cuprate high-temperature superconductors, which not only captures the fast vortices scenario at low density, but also predicts a novel mechanism of core-core collisions in dense vortex fluid regime. The theory clarifies the nature of vortex fluctuations being the quantum fluctuations of holes and then resolves a discrepancy of two orders of magnitude of Anderson's damping model $\hbar n_v$, with right prediction of the nonlinear field dependence of the resistivity $\rho = \rho_n(B + B_T)/(B_0 + B + B_T)$ and the Nernst effect, validated by data of several samples. Consequently, Anderson's vortex tangles concept and phase fluctuation scenario of pseudogap are verified quantitatively.

Recent experimental discoveries of the weak diamagnetism [1] and strong Nernst signal [2] above T_c have stimulated a hot debate about the presence of vortex liquid in pseudogap regime in high-temperature superconductivity (HTSC). A theoretically proposed fast-vortex scenario [3] is experimentally found [4] in dilute vortex regime, which is followed by a quick saturation in the magnetoresistance at high fields (knee feature) below T_c [2], or by a weak field dependence at high temperature in pseudogap state [5, 6]. The saturation is an unconventional behavior associated with dense vortex fluid, unable to be explained by isolated vortex scenario, nor by Bardeen-Stephen model [7] as well as the fast vortex theory [3]. In the dense vortex fluid, quasiparticle (qp) density of state (DOS) can be remarkably influenced by the overlapping of qp wave functions of neighboring vortices [8, 9], leading to an enhancement of qp scattering due to vortex-vortex interaction. This possibility was explored by Anderson with the idea of vortex tangles [10], but his estimated damping coefficient $\eta = \hbar n_v$ due to quantum fluctuations [11] presents an overestimation of two orders of magnitude compared to data. Moreover, current vortex fluid models and simulations can only account for the transverse thermoelectric coefficient $\alpha = e_N/\rho$ or Nernst signal, qualitatively. Thus, the legitimacy of the vortex liquid scenario and, more importantly the phase fluctuation explanation of pseudogap, calls for a refined quantitative damping model of vortex tangles.

In this letter, Anderson's idea of vortex tangles is extended to form a unified model for dilute and dense, magnetic and thermal vortex fluid. A novel damping mechanism of vortex tangles is proposed, which describes both the qp-defect scattering from isolated vortex and a novel core-core collisions of vortex entanglement. The new model clarifies the nature of the vortex fluid being the quantum fluctuations of holes, which resolves the discrepancy of Anderson's model, and describes quantitatively both the nonlinear field dependence of flux-flow resistivity $\rho = \rho_n(B + B_T)/(B_0 + B + B_T)$ and the Nernst

effect, as validated by data of several cuprate HTSC samples. Thus, a unified description of vortex transport in HTSC is achieved, establishing the legitimacy of Anderson's vortex tangles concept and phase fluctuation explanation of pseudogap [12].

We begin with a well-known picture of vortex fluid composed of pancake vortices, when a magnetic field is applied perpendicular to Cu-O plane on a cuprate superconductor. Once the temperature is higher than the critical temperature of Berezinskii-Kosterlitz-Thouless (BKT) phase transition [13], thermal vortices unbind, thus the vortex density $n_v = (B + B_T)/\phi_0$, where B_T is the characteristic field defined to describe the density of thermal vortices. When a vortex moves at a velocity v , the damping force is $f_d = \eta v$, where η is the damping coefficient. The resistivity due to damping transport of magnetic and thermal vortices is [14]

$$\rho = \frac{n_v}{\eta} \phi_0^2 c_0. \quad (1)$$

By the dimensional analysis,

$$\eta = \frac{m_p}{\tau}, \quad (2)$$

where m_p is the effective mass of the core and τ is the characteristic damping time. Both quantities will be estimated below based on our entangled vortex fluid model.

In a entangled vortex fluid, random motions of vortices are affected by three types of fluctuations: thermal fluctuations, quantum fluctuations of vortices, and quantum fluctuations of holes inside vortex cores. Their relative importance can be determined by the following energy estimates. The energy of quantum-fluctuations of vortices is $\epsilon_v = \hbar^2 n_v / 2m_p$, where the vortex effective mass m_p is defined as the bare hole mass inside the vortex core: $m_p = \pi \xi^2 n_h m_e$, with ξ the coherence length, n_h the two-dimensional hole density on Cu-O plane (multiply by layers), and m_e the electron mass. On the other hand, the energy associated with quantum fluctuations of holes is $\epsilon_h = \hbar^2 n_h / 2m_e$. Below, we express the three characteristic energy in terms of critical temperature T_c , critical vortex density $n_{c2} = H_{c2}/\phi_0$ and hole density; for instance, for optimal doped (OP) Bi₂Sr₂CaCu₂O_{8+ δ} (Bi-2212) [15, 16], $\epsilon_v = 0.84k_B \ll \epsilon_T = 90k_B \ll \epsilon_h = 478k_B$

* she@pku.edu.cn

(in Joule unit). This indicates that the fluctuations are dominated by quantum fluctuations of holes inside vortex cores. Using $\pi\epsilon_h$ in which a geometric factor π is considered, the random velocity is then found to be

$$v_R = \frac{\hbar}{m_e \xi}. \quad (3)$$

We propose that this speed controls the core-core collisions. Fig. 1 schematically shows the process of core-core collision: two vortex cores approach each other and merge into a bigger core due to qp wave-functions overlapping, leading to a decrease of intervals between the qp energy levels and the increase of low-energy DOS, as well as the enhancement of the qp-defect scattering inside the bigger core. Subsequently, the bigger core decompose into two cores which separate from each other. The critical vortex distance at which qp wave functions of neighboring vortices merge together is $\sqrt{2\pi}\xi$, i.e., at $B = H_{c2}$, but not the penetration depth λ according to the modified London equation [17]. The reason is that when the vortex distance l_v is much larger than $\sqrt{2\pi}\xi$, the influence of one vortex on the other do not change the qp wave functions inside vortex cores, and so do not contribute to dissipation. Thus, we define $\sqrt{2\pi}\xi$ as the core-core scattering length, below which the core-core collision takes place. This yields an estimate of the mean-free-path for a core-core collision as

$$l_c = 1/2\sqrt{2\pi}n_v\xi, \quad (4)$$

where we assume that the dissipation is similar for thermal and magnetic vortex. The characteristic time of core-core collision is then

$$\tau_c = \frac{l_c}{v_R} = \frac{m_e}{2\sqrt{2\pi}\hbar n_v}. \quad (5)$$

The momentum loss of two colliding vortices in one core-core collision determines the damping force, thus the damping coefficient η_c . Cuprate superconductors are doped Mott insulators in which plenty of defects (e.g., oxygen vacancies) exist on Cu-O plane [18], thus the relaxation time of qp scattering $\tau_q = m_e c_0 / n_h e^2 \rho_n$ is less than the core-core collision time τ_c in most regimes of vortex fluid phase except near H_{c2} , where c_0 is the lattice constant of c axis. For example, in OP Bi-2212, $\tau_q = 7.6 \times 10^{-14}$ s, and $\tau_c = B^{-1} 3.6 \times 10^{-12}$ s, indicating $\tau_q \leq \tau_c$ at $B \leq 47$ T. Therefore, it is reasonable to assume the transport momentum of two vortices totally disappear after one collision. This yields $\eta_c = m_p / \tau_c$. Eq. (3) and (5) yields

$$\eta_c = (2\pi)^{3/2} n_h \xi^2 \hbar n_v. \quad (6)$$

A comparison between Eq. (6) and Anderson's original model reveals the true physics of vortex tangles. Anderson proposed a vortex-vortex collision picture driven by quantum fluctuations of vortices (i. e. ϵ_v), predicting a damping coefficient $\eta = \hbar n_v$ with a random velocity $\hbar/m_p l_v$ and mean-free-path l_v [11]. Substitute it into the

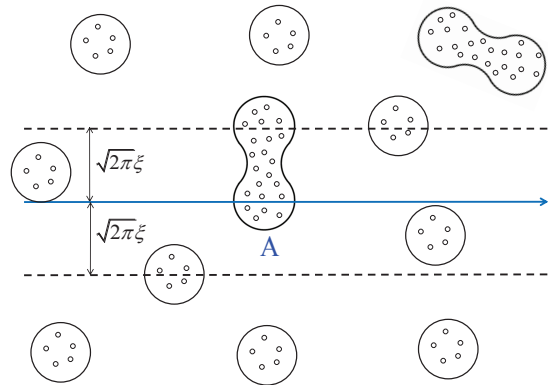


FIG. 1. Schematic diagram of core-core collisions. Vortex cores and qp are represented by big and small black circles, respectively. The qp DOS inside the isolate vortex core are small, thus should be described by a fast vortex scenario. On the other hand, in a core-core collision process, two vortex cores merge together to a bigger core which leads to an increase of qp DOS and damping. Two dash lines indicate that only the vortices the distance between which and the core trajectory (blue and solid line) is less than $\sqrt{2\pi}\xi$ participate in core-core collisions with vortex A.

resistivity formula Eq. (1), this yields $\rho = \rho_n = \hbar\phi_0^2 c_0$, independent of magnetic field, temperature and doping. A huge deficit arises since the predicted ρ_n (e. g., 126 $\mu\Omega\text{m}$ for any doping of Bi-2212) is nearly two orders of magnitude higher than experimental data (of Bi-2212) [6], see the red squares in Fig. 2. This discrepancy is now resolved in Eq.(6): a numerical factor $(2\pi)^{3/2} n_h \xi^2$ (equals 82 for OP Bi-2212) [2] is recovered due to the fact that the damping mechanism of vortex tangles is not driven by quantum fluctuations of vortices (as a whole) but by quantum fluctuations of holes inside the vortex cores.

At the dense vortices limit, core-core collisions dominate the damping coefficient, and ρ approaches the normal state resistivity,

$$\rho_n = \sqrt{\frac{\pi}{2}} \frac{c_0 H_{c2}}{e n_h}. \quad (7)$$

Qualitatively, H_{c2} shows a weak T dependence below and near T_c in HTSC [2], thus Eq. (7) predicts a constant ρ_n in this regime, which is consistent with data [19, 20]. Fig.2 shows the comparisons between theoretical predictions of Eq. (7) (taking H_{c2} reported in [1, 15, 20]) and the experimental data of ρ_n at the onset temperature at different doping [6, 19–21]. In making the prediction, the hole density n_h is set by $n_h = n * p * (a_0 * b_0)^{-1}$ with the layer number n , lattice constants a_0 and b_0 of the Cu-O plane [16], and hole concentration p which is estimated from the empirical formula $T_c(p) = T_{c,\text{max}}[1 - 82.6(p - 0.16)^2]$, where $T_{c,\text{max}}$ is the maximum T_c in one material [22]. The agreement

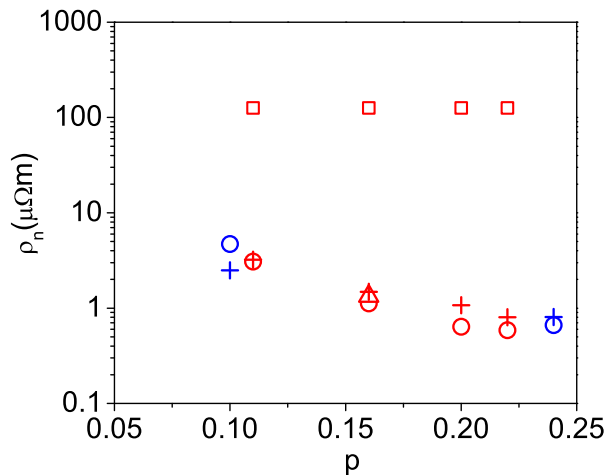


FIG. 2. ρ_n vs p (hole concentration) predicted with Eq. (7). The red and blue circles are from the experimental measurements of Bi-2212 [6], and Bi-2201 [19, 20] respectively, while the red triangle represents another sample of OP Bi-2212 [21]. The crosses are predictions of Eq. (7) with measured H_{c2} : red for Bi-2212 from Nernst signal [15], blue for Bi-2201 from diamagnetism [1] (at $p=0.10$, taking the data at $p=0.095$ as a approximation) and from magnetoresistance [20] (at $p=0.24$), respectively. The red squares are predictions from Anderson's damping model [11].

is very satisfactory with errors of the same order as the experimental uncertainty ($\pm 10\%$) of ρ_n and H_{c2} ; thus, the damping model of core-core collisions Eq. (6) is reliably verified. By the way, a more precise comparison requires the specification of the temperature dependence of H_{c2} and of the damping time τ (from τ_c), which will be discussed elsewhere.

Now, let us make a specific model for η . Generally speaking, three sources contribute to damping force, namely qp scattering from isolated vortex, the core-core collisions, and the pinning [23]. Therefore, η can be expressed as

$$\eta = \eta_0 + \eta_c + \eta_{pin}, \quad (8)$$

where η_0 represents qp-defect scattering from isolated vortex and is a material parameter independent of temperature and fields, η_c core-core collisions, and η_{pin} the pinning effect which is negligible in dense vortex fluid (e.g strong field or high temperature). Since η_0 is a constant, one can define an effective field B_0 so that

$$\eta_0 = B_0 \phi_0 c_0 / \rho_n. \quad (9)$$

According to Eq. (6) and (7), $\eta_c = n_v \phi_0^2 c_0 / \rho_n$. Combining Eq. (8) and (9) and neglecting the pinning effect, one can obtain

$$\rho = \rho_n \frac{B + B_T}{B_0 + B + B_T}. \quad (10)$$

Comparing to BS model [7], the extra terms $B + B_T$ in the denominator represent the damping effects due

to core-core collisions of magnetic and thermal vortices, thus ρ nonlinearly depends on vortex density. In Fig. 3, predictions of Eq. (10) (solid lines) are compared with the magnetoresistance data of overdoped (OD, $p=0.2$) $\text{La}_{2-x}\text{Sr}_x\text{CuO}_4$ (LSCO) below T_c and OP Bi-2212 in the pseudogap state [2, 21]. ρ_n used here is predicted with Eq. (7), and it is $0.68 \mu\Omega\text{m}$ for LSCO and $1.48 \mu\Omega\text{m}$ for OP Bi-2212. Since there is residual pinning effect indicated by melting field $H_m = 1.8 \text{ T}$ in OD LSCO, we assume that some vortices with a density H_m/ϕ_0 are pinned and can be simply subtracted, which leads to a substitution of $B + B_T$ with $B - H_m$ in Eq. (10).

As shown in Fig. 3, both the low-field steep rise and high-field rapid saturation of ρ are well captured by Eq. (10). In OD LSCO, since $\eta_0 = B_0 \phi_0 c_0 / \rho_n$, which is estimated to be only $1/38$ of the BS model (taking $H_{c2} \approx 46 \text{ T}$) [2], the fast vortices scenario is verified at low fields. The comparison also indicates that ρ saturates at high fields where η increases linearly and where the fast vortices scenario breaks down. Besides, data (circles) in pseudogap state of OP Bi-2212 [21] show two behaviors of field dependence of ρ corresponding to the dilute and dense thermal vortices limit. In the dilute thermal vortex limit, $\rho \approx \rho_n B / B_0$, the signal increases linearly with a large slope, from which B_0 can be determined. After B_0 is measured with the low-field signal, B_T can be determined from the zero-field signal with Eq. (10). Near T_c (where $B_T = 0$), ρ is determined by magnetic vortices only, thus sharply rises at low field. At $T = 105 \text{ K}$ ($> T_c \approx 85 \text{ K}$, with $B_T \approx 45 \text{ T}$), thermal vortices become dense and $B_T \gg B_0$, which leads to a saturation of ρ , thus the sample behaves metallic-like. This yields a complete picture of the vortex fluid in pseudogap state of HTSC, giving rise to the unconventional field dependence of ρ by Eq. (10), unifying both the fast vortices scenario and the vortex tangles with core-core collisions. In other words, the magnetoresistance signal in the phase fluctuations regime can be completely described by the current model of vortex tangles; no extra element is needed.

The damping model of vortex tangles, Eq. (6) and (8), can be applied to describe other anomalous transport phenomena in HTSC due to vortex motions. In the absence of a sound damping model in previous studies of Nernst signal in HTSC, only the transverse thermoelectric coefficient $\alpha_{xy} = e_N / \rho$ can be described [24]. The current damping model enables one to predict the Nernst signal quantitatively if a model of transport entropy is introduced. Using Anderson's proposal [11] and neglecting the pinning effect, we obtain [23]

$$e_N = C \frac{\rho_n n_s}{T} \frac{B \ln(H_{c2}/B)}{B_0 + B + B_T}. \quad (11)$$

where $C = \pi \hbar^2 / 8 m_e \phi_0 c_0$, n_s is the two-dimensional superfluid density on Cu-O plane and can be estimated from a linear model $n_s = n_{s0}(1 - T/T_v)$ where n_{s0} is the superfluid density at zero temperature, T_v is the onset temperature of vortex Nernst signal. Near and below T_c , H_{c2} is approximately constant, and $B_T =$

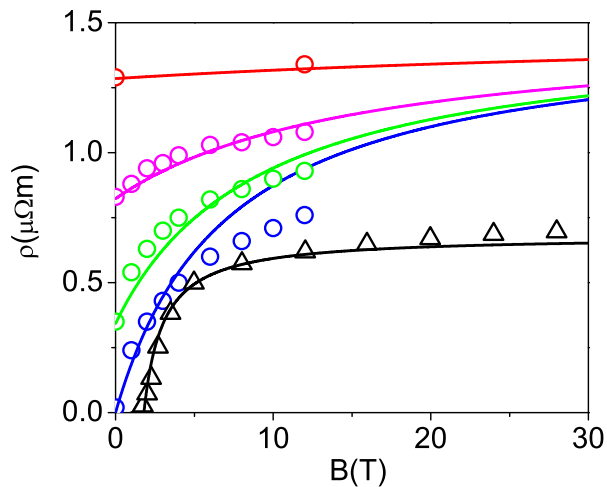


FIG. 3. The field dependence of ρ . Circles are data of OP Bi-2212 at $T = 85$ K (blue), 90 K (green), 95 K (magenta), 105 K (red) [21]. The black triangles are data of OD ($p=0.2$) LSCO at $T = 22$ K ($T_c=27$ K) [2]. Solid lines are predictions of Eq. (10).

$H_{c2} \exp[-2b(T/T_c - 1)^{-1/2}]$ as predicted by Korsterlitz [25]. As shown in Fig. 4, the magnitude of the Nernst signals in OD Bi-2212 [15] are quantitatively described by Eq. (11) for a range of B and T . In addition, Eq. (11) predicts correctly the peak shift from low to high fields when temperature increases, which is generated by the increase of thermal vortex density (by B_T in Eq.(11)). On the other hand, using the damping model of Anderson or the measurements based on fast vortices scenario [4, 11], the prediction will be two orders of magnitude higher than the data at high fields. We conclude that Nernst signal is also controlled by a damping increase from low to high fields due to vortex tangles, for which our damping model, i.e., Eq. (8), is suitable for quantitative descriptions.

In summary, Anderson's vortex tangles concept and phase fluctuation explanation of pseudogap are verified in a quantitative manner. We go beyond the picture of isolated vortices [7, 14] with a novel model of vortex tangles, predicting both flux-flow resistivity and Nernst signal in cuprate superconductors. Since vortex damping

mechanism is the key factor of vortex transport, the current model opens several new avenues for further studies. First, the model can be extended to describe Fe-based HTSC due to a similar dirty metal nature. Secondly, distinct from the static calculation with Bogoliubov-de Gennes (BdG) equations [8, 9], the new scenario of core-core collision is a dynamic mechanism, which has implications for the further development of microscopic theories, such as the collision enhancement of qp DOS with a model of vortex-distance fluctuations in qp tunneling calculation. Thirdly, this work suggests that a realistic simulation of vortex fluid at arbitrary T and B by a time-dependent Ginzburg-Landau (TDGL) equation [26–28] is feasible, if a field and temperature dependent relaxation

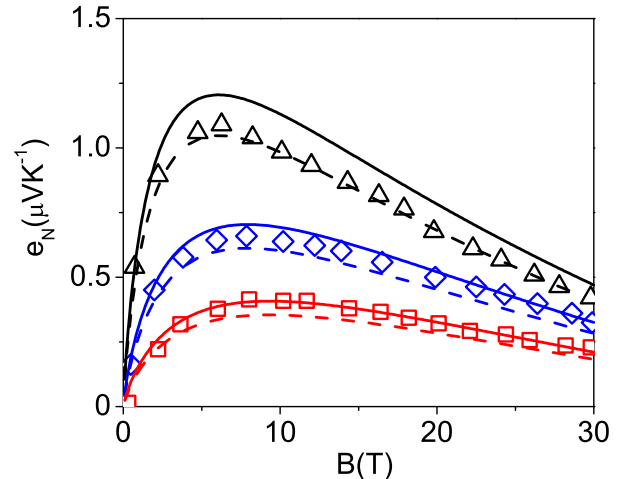


FIG. 4. e_N vs B at three different temperatures $T_c=65$ K (black), 67.5 K (blue), 70 K (red)). Symbols are data in OD ($p=0.22$) Bi-2212 [15]. Solid lines and dash lines are predictions of Eq. (11) at $n_{s0} = n_h/2$ and $n_h/2.3$, respectively. The other parameters are $T_v = 77.3$ K (estimated from the onset temperature of e_N), $\rho_n = 0.803 \mu\Omega\text{m}$ (predicted with Eq. (7), see also Fig. 2), and $H_{c2} = 50$ T (estimated from zero point of e_N), $B_0 = 5.5$ T (determined from low field signal at $T = 65$ K) and $b=0.25$.

time is introduced to capture the dissipation of vortex tangles. Finally, vortex entanglement may yield exotic transport phenomena such as heat transfer in Ettingshausen effects [29] and anomalous thermal conductivity in HTSC [30].

[1] L. Li, Y. Wang, S. Komiya, S. Ono, Y. Ando, G. D. Gu, and N. P. Ong, Phys. Rev. B **81**, 054510 (2010).
 [2] Y. Wang, L. Li, and N. P. Ong, Phys. Rev. B **73**, 024510 (2006).
 [3] L. B. Ioffe and A. J. Millis, Phys. Rev. B **66**, 094513 (2002).
 [4] L. S. Bilbro, R. Valdés Aguilar, G. Logvenov, I. Bozovic, and N. P. Armitage, Phys. Rev. B **84**, 100511 (R) (2011); G. Wachtel and D. Orgad, Phys. Rev. B **90**, 184505

(2014).
 [5] P. A. Lee, N. Nagaosa, and X.-G. Wen, Rev. Mod. Phys. **78**, 17 (2006).
 [6] T. Usui, D. Fujiwara, S. Adachi, H. Kudo, K. Murata, H. Kushibiki, T. Watanabe, K. Kudo, T. Nishizaki, N. Kobayashi, S. Kimura, K. Yamada, T. Naito, T. Noji, and Y. Koike, J. Phys. Soc. Jpn. **83**, 064713 (2014).
 [7] J. Bardeen and M. J. Stephen, Phys. Rev. **140**, A 1197 (1965).

- [8] A. S. Mel'nikov and M. A. Silaev, JETP Lett. **83**, (2006).
- [9] E. Canel, Phys. Lett. **16**, 101 (1965).
- [10] P. W. Anderson, Phys. Rev. Lett. **96**, 017001 (2006); P. W. Anderson, Nat. Phys. **3**, 160 (2007).
- [11] P. W. Anderson, arXiv: 0603726 (unpublished).
- [12] V. J. Emery and S. A. Kivelson, Nature (London) **374**, 434 (1995).
- [13] V. L. Berezinskii, Zh. Eksp. Teor. Fiz. **61**, 1144 (1972), [Sov. Phys. JETP **34**, 610 (1972)]; J. M. Kosterlitz and D. J. Thouless, J. Phys. C **5**, L124 (1972); J. M. Kosterlitz and D. J. Thouless, J. Phys. C **6**, 1181 (1973).
- [14] B. I. Halperin and D. R. Nelson, J. Low. Temp. Phys. **36**, 599 (1979).
- [15] Y. Wang, S. Ono, Y. Onose, G. Gu, Y. Ando, Y. Tokura, S. Uchida, and N. Ong, Science **299**, 86 (2003).
- [16] W. Zhou and W. Liang, *Fundamental Research of High-temperature superconductor* (Shanghai Science Press, Shanghai, 1999).
- [17] M. Tinkham, *Introduction to superconductivity*, 2nd ed. (McGraw-Hill, New York, 1996).
- [18] G. Blatter, M. V. Feigel'man, V. B. Geshkenbein, A. I. Larkin, and V. M. Vinokur, Rev. Mod. Phys. **66**, 1125 (1994).
- [19] Y. Z. Zhang, R. Deltour, J.-F. de Marneffe, Y. L. Qin, L. Li, Z. X. Zhao, A. G. M. Jansen and P. Wyder, Phys. Rev. B **61**, 8675 (2000).
- [20] Y. Ando, G. S. Boebinger, A. Passner, N. L. Wang, C. Geibel, and F. Steglich, Phys. Rev. Lett. **77**, 2065 (1996).
- [21] H.-C. Ri, R. Gross, F. Gollnik, A. Beck, R. P. Huebener, P. Wagner, and H. Adrian, Phys. Rev. B **50**, 3312 (1994).
- [22] S. D. Obertelli, J. R. Cooper, and J. L. Tallon, Phys. Rev. B **46**, 14928 (1992).
- [23] R. Li and Z. S. She, arXiv: 1701.01832 (unpublished).
- [24] I. Ussishkin, S. L. Sondhi, and D. A. Huse, Phys. Rev. Lett. **89**, 287001 (2002); D. Podolsky, S. Raghu, and A. Vishwanath, Phys. Rev. Lett. **99**, 117004 (2007).
- [25] J. M. Kosterlitz, J. Phys.C: Solid St. Phys. **6**, 1046 (1974).
- [26] M. Machida and H. Kaburaki, Phys. Rev. Lett. **71**, 3206 (1993).
- [27] W. Kwok, U. Welp, A. Glatz, A. E. Koshelev, K. J. Kihlstrom, and G. W. Crabtree, Rep. Prog. Phys. **79**, 116501 (2016).
- [28] S. Mukerjee and D. A. Huse, Phys. Rev. B **70**, 014506 (2004).
- [29] T. T. M. Palstra, B. Batlogg, L. F. Schneemeyer, and J. V. Waszczak, Phys. Rev. Lett. **64**, 3090(1990).
- [30] G. Grissonnanche, O. Cyr-Choinière, F. Laliberté, S. René de Cotret, A. Juneau-Fecteau, S. Dufour-Beauséjour, M.-E. Delage, D. LeBoeuf, J. Chang, B. J. Ramshaw, D. A. Bonn, W. N. Hardy, R. Liang, S. Adachi, N. E. Hussey, B. Vignolle, C. Proust, M. Sutherland, S. Kramer, J.-H. Park, D. Graf, N. Doiron-Leyraud, and L. Taillefer, Nat. Commun. **5**, 3280 (2014).